Filamin A controls matrix metalloproteinase activity and regulates cell invasion in human fibrosarcoma cells

Massimiliano Baldassarre[1,*], Ziba Razinia[1], Nina N. Brahme[1], Roberto Buccione[2] and David A. Calderwood[1,*]

[1]Department of Pharmacology, Department of Cell Biology and Interdepartmental Program in Vascular Biology and Therapeutics, Yale University School of Medicine, New Haven, CT 06520-8066, USA
[2]Tumor Cell Invasion Laboratory, Consorzio Mario Negri Sud, Santa Maria Imbaro, Chieti 66030, Italy
*Authors for correspondence (massimiliano.baldassarre@yale.edu; david.calderwood@yale.edu)

Accepted 12 April 2012
Journal of Cell Science 125, 3858–3869
© 2012. Published by The Company of Biologists Ltd
doi: 10.1242/jcs.104018

Summary

Filamins are an important family of actin-binding proteins that, in addition to bundling actin filaments, link cell surface adhesion proteins, signaling receptors and channels to the actin cytoskeleton, and serve as scaffolds for an array of intracellular signaling proteins. Filamins are known to regulate the actin cytoskeleton, act as mechanosensors that modulate tissue responses to matrix density, control cell motility and inhibit activation of integrin adhesion receptors. In this study, we extend the repertoire of filamin activities to include control of extracellular matrix (ECM) degradation. We show that knockdown of filamin increases matrix metalloproteinase (MMP) activity and induces MMP2 activation, enhancing the ability of cells to remodel the ECM and increasing their invasive potential, without significantly altering two-dimensional random cell migration. We further show that within filamin A, the actin-binding domain is necessary, but not sufficient, to suppress the ECM degradation seen in filamin-A-knockdown cells and that dimerization and integrin binding are not required. Filamin mutations are associated with neuronal migration disorders and a range of congenital malformations characterized by skeletal dysplasia and various combinations of cardiac, craniofacial and intestinal anomalies. Furthermore, in breast cancers loss of filamin A has been correlated with increased metastatic potential. Our data suggest that effects on ECM remodeling and cell invasion should be considered when attempting to provide cellular explanations for the physiological and pathological effects of altered filamin expression or filamin mutations.

Key words: ECM, Filamin, Matrix metalloproteinase, MMP, TIMP

Introduction

Filamins (FLNs) are an important family of conserved actin-binding proteins with essential roles in development, tissue formation and morphogenesis, and mechanosensing (Yamazaki et al., 2002; Kim and McCulloch, 2011; Razinia et al., 2012). Vertebrate FLNs are non-covalent homodimers of 240–280 kDa subunits composed of an N-terminal actin-binding domain followed by 24 immunoglobulin-like (IgFLN) domains, the last of which mediates dimerization (Gorlin et al., 1990; Pudas et al., 2005). Dimerization results in a V-shaped molecule. Two hinge regions, between IgFLN domains 15 and 16 (hinge 1), and 23 and 24 (hinge 2), add flexibility to the molecule making it capable of linking and stabilizing orthogonal networks with high-angle F-actin branching (Hartwig et al., 1980). FLNs also bind many transmembrane receptors, signaling and adapter proteins (Feng and Walsh, 2004; Popowicz et al., 2006; Stossel et al., 2001) and it is believed that in addition to direct effects on actin crosslinking, FLNs function through assembly of networks linking receptors with signaling molecules and the actin cytoskeleton and so can regulate a range of cellular activities (Stossel et al., 2001).

Humans have three FLN-encoding genes, filamin A (FLNa), filamin B (FLNb) and filamin C (FLNc). Of these, FLNa is the most abundant and broadly expressed, FLNb is also widely expressed, while FLNc is largely restricted to striated muscle (van der Flier and Sonnenberg, 2001; Stossel et al., 2001). The three FLNs have both overlapping and independent functions and activities (Kesner et al., 2010) and truncations or missense mutations in any of the three human FLNs have been associated with a wide spectrum of congenital anomalies including malformations of the skeleton, brain, muscle and cardiovascular system (Nakamura et al. 2011; Robertson et al., 2003; Zhou et al., 2007; Zhou et al., 2010). It is assumed that alterations in interactions with specific FLN-binding partners and consequent perturbation of cytoskeletal and signaling networks underlies these pathologies but their molecular bases remain unknown.

In addition to diseases associated with germline changes in FLN genes, FLN mutations have also been identified in human breast and colon cancers (Nakamura et al., 2011). A major cause of death in cancer patients is the development of metastatic secondary tumors in distal organs. Metastasis is a complex process during which tumor cells become invasive, migrating away from the primary tumor and passing through natural extracellular matrix (ECM)-based barriers impeding access to vascular or lymphatic vessels. Cell invasion is a multi-faceted process requiring the integration of several basic processes including, at the cellular level, cell migration, adhesion and pericellular ECM degradation and remodeling, and at the

Journal of Cell Science

subcellular level local modulation of cytoskeletal structure, and contractile forces and delivery and activation of ECM degrading enzymes. In this context, F-actin-binding protein such as filamins (FLNs) that anchor the actin cytoskeleton to adhesion receptors and therefore to the ECM are likely to play crucial roles. To date, however, the focus on FLNs has been largely restricted to effects on cell motility and cytoskeletal and membrane dynamics rather than ECM remodeling.

A central role for filamins in cell migration was initially proposed based on motility defects in FLNa-deficient melanoma cells (Cunningham et al., 1992). This was further supported by indications that FLNa-deficiency impaired neuronal migration (Fox and Walsh, 1999; Nagano et al., 2002). Further studies based on knockout mice (Hart et al., 2006; Feng et al., 2006) and the use of small interference RNA showed that while in many settings loss of only one FLN isoform is not sufficient to impair migration, loss of two or more FLNs impaired initiation of migration and cell spreading (Baldassarre et al., 2009; Lynch et al., 2011; Heuzé et al., 2008). Surprisingly, two recent studies found that FLNa expression negatively correlates with the ability of breast cancer cells to invade and disseminate (Xu et al., 2010; Caruso and Stemmer, 2011). Thus, despite its roles in cell migration, at least in some settings FLNa deficiency can increase the ability of tumor cells to escape from the primary tumor and metastasize to distal organs.

Using shRNA mediated FLN knockdown in HT1080 human fibrosarcoma cells we now report that loss of FLNa leads to a decrease of tissue inhibitor of metalloproteinase 2 (TIMP-2) secretion and an increase of maxtrix metalloproteinase (MMP) activity, MMP2 activation, increased pericellular matrix degradation, and enhanced cell invasion. These unanticipated effects of FLN on proteolytic remodeling of the ECM provide a potential mechanism for the reported consequences of FLNa-deficiency in tumor cell metastasis.

Results

Loss of filamin enhances ECM degradation in HT1080 cells

To study the role of FLNa in extracellular matrix remodeling we used a previously established HT1080 cell line stably transfected with an shRNA against human FLNa (FLNaKD; Baldassarre et al., 2009). These cells feature very low levels of FLNa (5% of the original line levels) (Fig. 1A) with no changes in FLNb or integrin β1 levels and no dramatic effects on the actin cytoskeleton (Baldassarre et al., 2009). To study ECM degradation, we took advantage of a well-established assay (Baldassarre et al., 2003; Mueller and Chen, 1991). In this experimental approach, cells are plated on glass coverslips coated with a thin layer of cross-linked fluorescent gelatin. ECM degradation is visualized as dark areas where the fluorescent gelatin has been removed from the coverslip. Quantification of ECM degradation is carried out by measuring the area of degradation under and in the vicinity of each cell (as described in Materials and Methods). The values obtained are expressed as total degradation area per cell and are thus a direct readout of degradation ability that accounts for most foreseeable variables (i.e. total number of cells, number of degrading cells, number of degradations per cell and the size of each region of degradation).

When plated on fluorescent gelatin coated coverslips, wild-type HT1080 cells slowly degrade the fluorescent matrix and after 4 hours only a few degradations are present (Fig. 1B, upper panel). In contrast, at the same time point HT1080 cells lacking filamin A (FLNaKD) exhibit larger areas of degradation (Fig. 1B, lower panel). As shown in Fig. 1C, FLNaKD cells degraded significantly more gelatin per cell than wild-type cells.

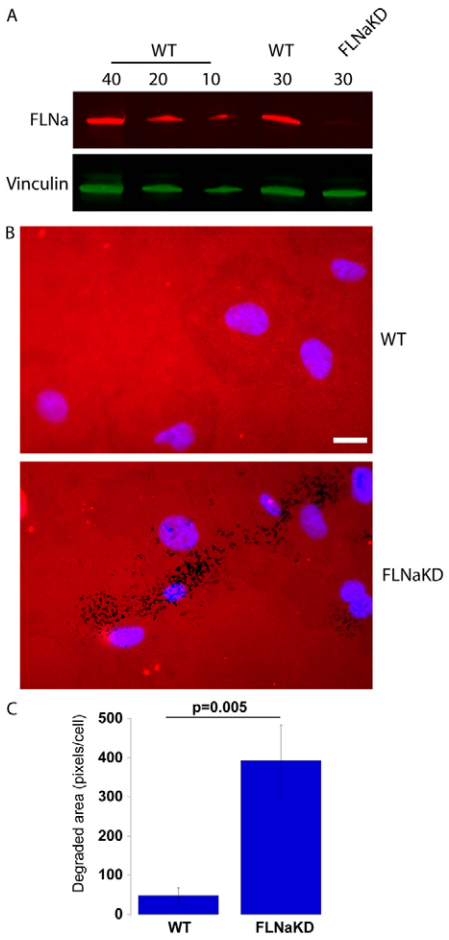

Fig. 1. Knockdown of FLNa in HT1080 increases ECM degradation. (**A**) FLNa expression in FLNaKD cells was quantified by immunoblotting comparing 30 μg of cell lysate with a curve of cell lysates prepared from HT1080 WT cells. Vinculin expression was used as loading control. Blots were imaged using a LI-COR Odyssey Imaging system. (**B**) HT1080 WT (upper panel) or FLNaKD (lower panel) cells were plated on cross-linked fluorophore-conjugated gelatin for 4 hours, fixed, stained with DAPI to label the nuclei and analyzed at the microscope. Scale bar: 20 μm. (**C**) The degradation under the cells was quantified as described in the Materials and Methods, and the area per cell was plotted (mean±s.e.m.; sample size of >2000 cells in six independent experiments).

To further characterize the differences between wild-type (WT) and FLNaKD cells we performed a time course experiment and measured mean degradation area per cell over the course of 6 hours. As shown in Fig. 2A, removal of FLNa increases the total area of degradation at all time points examined. This increase could be due to an increase in the percentage of cells that degrade the matrix, in the number of degradation events per cell, in the area of each degradation event or combinations of these effects. As shown in Fig. 2B, the number of degrading cells is higher in FLNaKD cells, in fact after 1 hour most FLNaKD cells (95%) present at least one degradation, while less than half of the HT1080 cells do. In addition, if we only consider cells with detectable degradations we find that the FLNaKD cells have

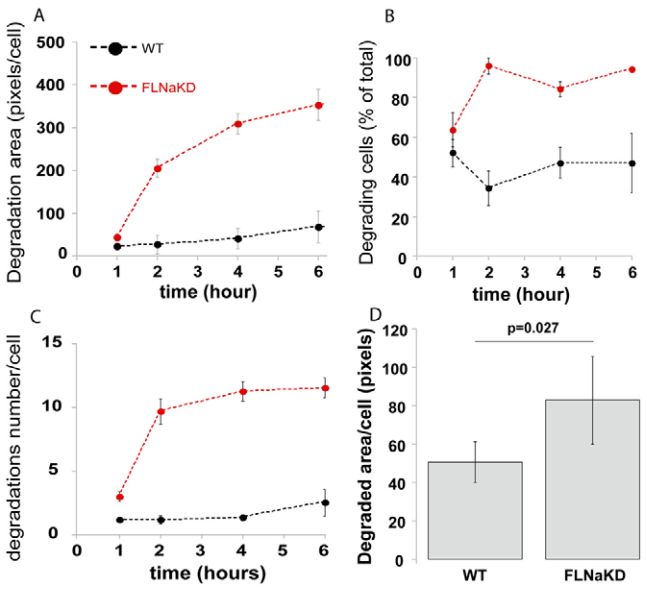

Fig. 2. FLNa knockdown enhances the frequency of ECM degradation events. (**A–C**) WT or FLNaKD HT1080 cells were plated on cross-linked fluorophore-conjugated gelatin for the indicated time, fixed and stained with DAPI. (A) The mean (±s.e.m.) degradation area per cell was calculated as in Fig. 1 and plotted for each time point. (B) The percentage of cells with at least one degradation of greater than 4 pixels was measured and plotted for each time point. (C) In cells with at least one degradation, the mean number of degradations was quantified and plotted at each time point. Plots are mean ±s.e.m. for >50 cells per time point in three independent experiments. (**D**) WT or FLNaKD HT1080 cells were plated on cross-linked fluorophore-conjugated fibronectin for 6 hours, fixed, stained with DAPI to label the nuclei, and analyzed at the microscope to measure degradation areas. Results are means±s.e.m. (sample size of >45 cells) for three independent experiments.

increased numbers of degradations per cell (Fig. 2C). Thus the increased gelatin degradation observed in FLNaKD HT1080 cells is due to both an increased number of degrading cells and area of degradation in these cells.

Finally, to verify whether degradation was specific for gelatin we repeated the assay plating the cells on fluorescent fibronectin. As expected, fibronectin, which in comparison to gelatin is a native folded protein, required longer incubation times to reveal detectable degradation. Nevertheless, the HT1080 FLNaKD cells degrade fibronectin more extensively than the wild-type parental line (Fig. 2D) confirming that the increased degradation ability is not restricted to gelatin.

HT1080 cells express both FLNa and FLNb (Baldassarre et al., 2009). To determine whether FLNb plays a similar role to FLNa in ECM degradation we used a previously established HT1080 cell line stably transfected with an shRNA against human FLNb (FLNbKD) and we confirmed the specificity of the shRNAs measuring FLNa levels in FLNbKD cells and vice versa (Baldassarre et al., 2009) (Fig. 3A). Consistent with our observations in FLNaKD cells, we found an increase in gelatin degradation in the FLNbKD cells (Fig. 3B). This effect was significant ($P=0.047$), but the magnitude of the increase in degradation was less that that observed in FLNaKD cells. This is in keeping with our observation that FLNa is more abundant than FLNb in HT1080 cells (Baldassarre et al., 2009). Nonetheless, this result establishes that both FLNa and FLNb can increase

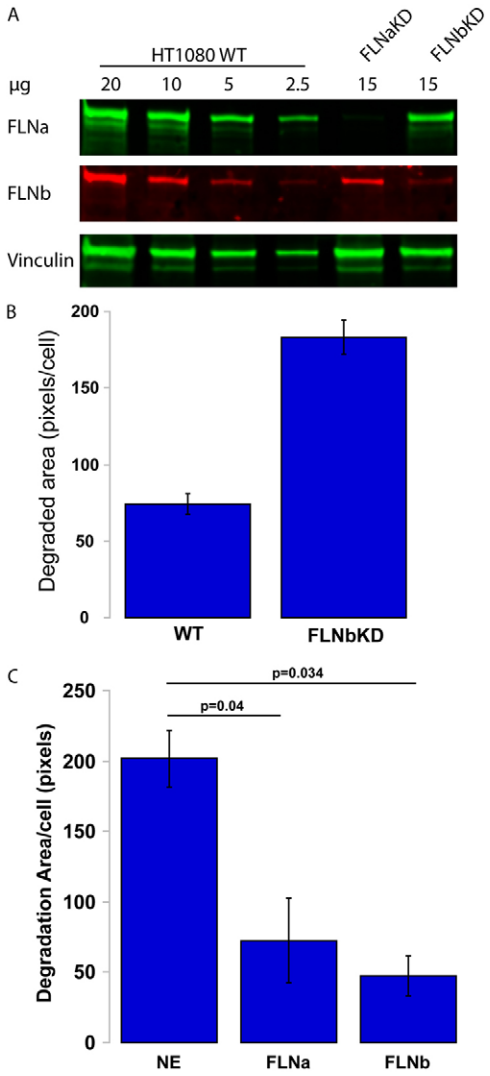

Fig. 3. FLNb knockdown enhances ECM degradation. (**A**) Specificity of shRNAs for the two isoforms of FLNa was assessed by immunoblotting and measuring expression levels of FLNa (top panel) and FLNb (middle panel) in FLNaKD and FLNbKD HT1080 cells. Vinculin expression (lower panel) was used as the loading control. Signals from all three proteins were imaged simultaneously on the same membrane using a LI-COR Odyssey Imaging system. (**B**) HT1080 WT or FLNbKD cells were plated on cross-linked fluorophore-conjugated gelatin for 4 hours, fixed, stained with DAPI to label the nuclei and analyzed at the microscope. The degradation area under the cells was quantified as described in the Materials and Methods. Results are means±s.e.m. (sample size of >300 cells in three independent experiments). (**C**) HT1080 FLNaKD cells were transfected with FLNa-GFP or FLNb-GFP then plated on cross-linked fluorophore-conjugated gelatin for 4 hours, fixed, stained with DAPI to label the nuclei and analyzed at the microscope. The degradation area under the cells was quantified as described in the Materials and Methods, degradations under the transfected (green) cells were compared with those under the non-expressing (NE) cells on the same coverslip. Results are means±s.e.m. (sample size of >30 cells in three independent experiments).

ECM degradation, and very strongly suggests that the effects observed in the FLNaKD line are not due to off-target mutations acquired during selection of the FLNaKD cell line but rather reflect a general FLN-dependent process. More importantly, the enhanced degradation in FLNaKD cells was reverted when cells

were transfected with FLNa or FLNb (Fig. 3C), indicating that changes in the total level of FLN, rather than the expression of specific isoforms, is probably responsible for the effect on ECM degradation.

Altered cell migration does not account for the increase in ECM degradation by FLNaKD cells

Filamins have been implicated in cell migration and stationary or poorly motile cells would typically have more time to degrade the ECM in a given area; hence it is possible that a migration defect could indirectly lead to an increase in ECM degradation. We have previously shown that FLNaKD HT1080 cells do not have measurable migration defects when plated on fibronectin (Baldassarre et al., 2009); but since most of our degradation assays are performed on cross-linked gelatin, we compared random migration of WT and FLNaKD cells in this setting. As illustrated in supplementary material Fig. S1 and Movie 1, we confirmed that under these conditions down-regulation of FLNa does not affect HT1080 migration. Hence, augmented degradation consequent to FLNa knockdown cannot be ascribed to defective migration.

Filamin knockdown increases matrix metalloproteinase activity

The cross-linked fluorescent matrix used in our experiments is insoluble and very stable, and only aggressive, protease-secreting cells are expected to effectively degrade it. Secreted or cell surface MMPs are the major family of enzymes implicated in proteolytic remodeling of the ECM during tumor progression (Kessenbrock et al., 2010). To test whether metalloproteinase activity is required for the enhanced degradation observed in FLNaKD HT1080 cells, we treated cells with the broad-specificity metalloproteinase inhibitor GM6001 (Grobelny et al., 1992). As illustrated in Fig. 4A, this almost completely abolished the ability of HT1080 FLNaKD to degrade the substrate, showing that FLNa knockdown enhances metalloproteinase-dependent ECM degradation and suggesting that filamin knockdown may increase metalloproteinase activity. To test this directly, we used a flurogenic substrate based assay (Knight et al., 1992) that relies on a quenched fluorescent peptide; MMP-dependent proteolysis of the peptide separates the fluorophore from the quencher enhancing fluorescence. When we assessed MMP activity in serum-free media conditioned by wild-type or FLNaKD cells we found increased MMP activity in FLNaKD cells (Fig. 4B). The broad-specificity metalloproteinase inhibitor GM6001 strongly inhibits proteolysis confirming the specificity of the assay. The slope of the trend-line provides a measure of proteolysis rate and quantification of 9 replicates in 3 independent experiments revealed that FLNaKD cells exhibit a 39.5±5.5% increase in rate of degradation ($P<0.001$). The peptide used in this assay is a general MMP substrate albeit with some selectivity for MMP2 and MMP9 (Neumann et al., 2004). To identify the MMPs potentially involved in the enhanced ECM degradation in FLNaKD cells we performed a zymographic analysis on serum-free media conditioned by WT or FLNaKD cells. The two major matrix metalloproteinases secreted by HT1080 are MMP9 and MMP2 (Stanton et al., 1998) and indeed we detected activity at molecular weights consistent with these proteins in conditioned medium from both WT and FLNaKD cells (Fig. 4C). We did not, however, detect any significant difference in the total levels of the two MMPs between WT and FLNaKD cells (Fig. 4D,E). On the other hand, while we only detected the inactive immature form of MMP9 in the conditioned media, MMP2 was found to be partially activated, as suggested by the presence of a lower molecular weight species consistent with that of the mature form (Fig. 4C). More importantly, FLNaKD cells presented an almost 5-fold increase in MMP2 activation (from ~10% in wild-type cells to ~45% in FLNaKD cells) (Fig. 4F). To confirm that MMP2 activation was due to FLNa knockdown and not to an off-target effect, we selected two independent lines of FLNaKD HT1080 cells re-expressing FLNa. In these cells MMP2 activation was reverted to WT levels (Fig. 4F), confirming that the effect is FLNa dependent.

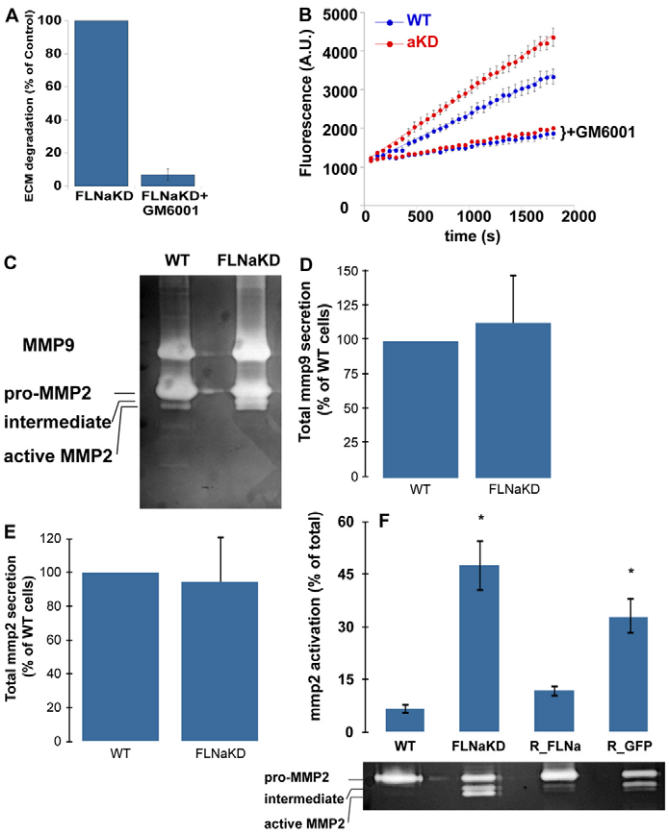

Fig. 4. Filamin knockdown increases matrix metalloproteinase activity. (**A**) FLNaKD HT1080 cells were plated on cross-linked fluorophore-conjugated gelatin for 4 hours in the presence or absence of 50 μm GM6001, fixed, stained with DAPI to label the nuclei. Degradation was analyzed as in Fig. 1 and the mean (±s.e.m.) degradation, normalized to the untreated control, is plotted (>75 cells from four independent experiments). (**B**) MMP activity in serum-free conditioned medium from WT or FLNaKD cells was assessed using a fluorogenic substrate peptide. A representative experiment shows the fluorescence at each time point (mean±s.e.m.) in the absence or presence of MMP inhibitor. Specific signal was measured, subtracting the background (+GM6001) from the measured point. (**C**) Representative zymogram of 24 hour-conditioned medium from HT1080 WT or FLNaKD cells. (**D**) Quantification of total levels of MMP9. Results are means±s.e.m. for six independent zymograms. (**E**) Quantification of total levels of MMP2 (pro-MMP2+intermediate+mature MMP2). Results are means±s.e.m. for six independent zymograms. (**F**) Lower panel: zymogram of 24-hour conditioned medium from WT, FLNaKD, or FLNaKD HT1080 cells rescued with FLNa (R_FLNa) or GFP (R_GFP). Upper panel: quantification representing the mean of four experiments (±s.e.m.). *$P<0.05$ when compared with WT cells.

Loss of FLNb also enhances ECM degradation (Fig. 3B), and consistently FLNbKD HT1080 cells exhibit a 20.5±6.1% increase in rate of degradation ($P<0.001$) of the fluorogenic MMP substrate peptide. Furthermore, as for FLNaKD cells, zymography of serum-free conditioned medium (Fig. 5A) shows that FLNbKD cells have significantly increased MMP2 activation with no alteration in total levels of secreted MMP2 or MMP9 (Fig. 5B,C,D). In addition to MMPs secreted by HT1080 cells, matrix degradation can be mediated by MMPs present in the serum that can be activated in a cell-dependent manner. Our matrix degradation assays (Figs 1–3) were performed in the presence of serum while enzymatic activity and zymography assays (Figs 4, 5) were performed in serum-free medium. To test whether cell-derived MMPs are sufficient to drive gelatin degradation we therefore repeated our fluorescent ECM degradation assays in the absence of serum. As shown in Fig. 5E, even in absence of serum-derived exogenous proteases, HT1080 FLNaKD and FLNbKD cells exhibit higher levels of ECM degradation than the wild-type filamin-expressing cells. Furthermore, re-expression of FLNa in FLNaKD or FLNb in FLNbKD cells rescues the degradation phenotype under these conditions (Fig. 5E). Thus, loss of either FLNa or FLNb increases both ECM degradation and MMP2 activation.

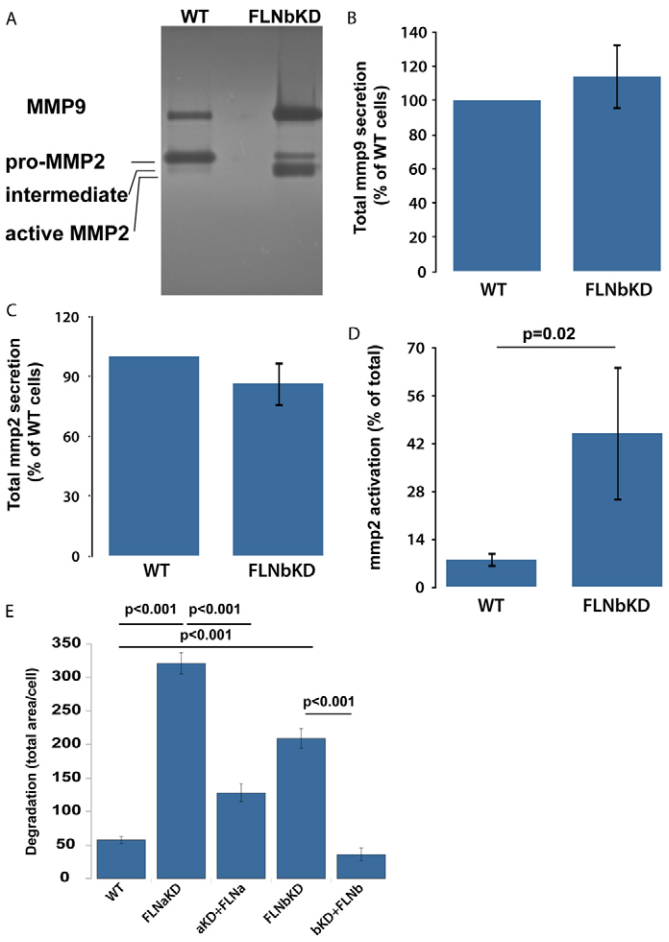

Fig. 5. FLNbKD increases MMP2 activation without affecting its expression levels. (**A**) Representative image from a real-time zymogram (16-hour incubation time) of 24-hour-conditioned medium from HT1080 WT or FLNbKD cells. (**B**) Quantification of total levels of MMP9. Results are means±s.e.m. for six independent zymograms. (**C**) Quantification of total levels of MMP2 (pro-MMP2+intermediate+mature MMP2). Results are means±s.e.m. for six independent zymograms. (**D**) Zymogram of 24-hour-conditioned medium from HT1080 WT or FLNbKD cells. Results are means±s.e.m. for four experiments. (**E**) WT, FLNaKD or FLNbKD HT1080 cells were transfected or not with FLNa-GFP or FLNb-GFP, then plated on cross-linked fluorophore-conjugated gelatin in absence of serum for 5 hours, fixed, stained with DAPI to label the nuclei, and analyzed at the microscope. Quantification represents the mean of at least 167 cells from three independent experiments.

Enhanced MMP2 activation in FLNaKD cells is not due to increased MT1-MMP activation

MMP2 activation is known to be mediated by membrane-type MMPs (MT-MMPs) rather than soluble proteinase cascades (Ra and Parks, 2007). Intriguingly, probably the most relevant one in this context, MT1-MMP, is activated by cleavage by furin and other pro-convertases (Mazzone et al., 2004; Ra and Parks, 2007), and FLNa has been implicated in furin trafficking (Liu et al., 1997). Since HT1080 cells express MT1-MMP, we analyzed whether FLNa knockdown affects its expression and/or processing. Total cell lysates from WT or FLNaKD HT1080 were analyzed by western blotting using an antibody against the catalytic domain of MT1-MMP. As shown in Fig. 6A, this antibody recognizes a major band around 57 KD, consistent with the molecular weight of mature MT1-MMP. A minor band around 62 KD, the pro-MT1-MMP, is also visible just above the prominent band. A third non-active, 44 KD, molecular form lacking the catalytic domain has also been described for MT1-MMP (Stanton et al., 1998); obviously the antibody we used cannot detect this form. As shown in the representative blot in Fig. 6A and the quantification of 6 independent experiments in Fig. 6B, there was no difference in the total amount (mature + pro-form) of MT1-MMP expression between HT1080 WT and HT1080 FLNaKD. Similarly no differences in cell-surface MT1-MMP were detected by flow cytometry (Fig. 6C). More importantly, when we compared the percentage of mature MT1-MMP in the two different lines, we found no increase in MT1-MMP activation in FLNaKD cells (Fig. 6D). Indeed we observed a small but consistent and statistically significant ($P=0.03$, $n=6$) decrease in mature MT1-MMP in FLNaKD (Fig. 6D). It is unclear whether such a small decrease would be biologically relevant, but in any case it is very unlikely that a decrease in MT1-MMP activation would lead to increased MMP2 activation. In conclusion, FLNa knockdown enhances MMP-dependent matrix degradation and increases MMP2 activation without increasing MT1-MMP processing.

Filamin knockdown decreases TIMP-2 secretion

MMP2 activation is an intricate process controlled by both activators and inhibitors (Ra and Parks, 2007). Notably, tissue inhibitor of metalloproteinase 2 (TIMP-2) is unique as by binding both MT1-MMP and MMP2 it can serve as an inhibitor or activator of MMP2 (Sato and Takino, 2010; Bourboulia and Stetler-Stevenson, 2010). TIMP-2 tethers MMP2 to cells via MT1-MMP increasing its activation by free MT1-MMP, but TIMP-2 also inhibits the enzymatic activity of MT1-MMP impairing MMP2 activation. Which of these functions is dominant is determined by the concentration of TIMP-2 in the medium: high TIMP-2 levels inhibit MT1-MMP, and other

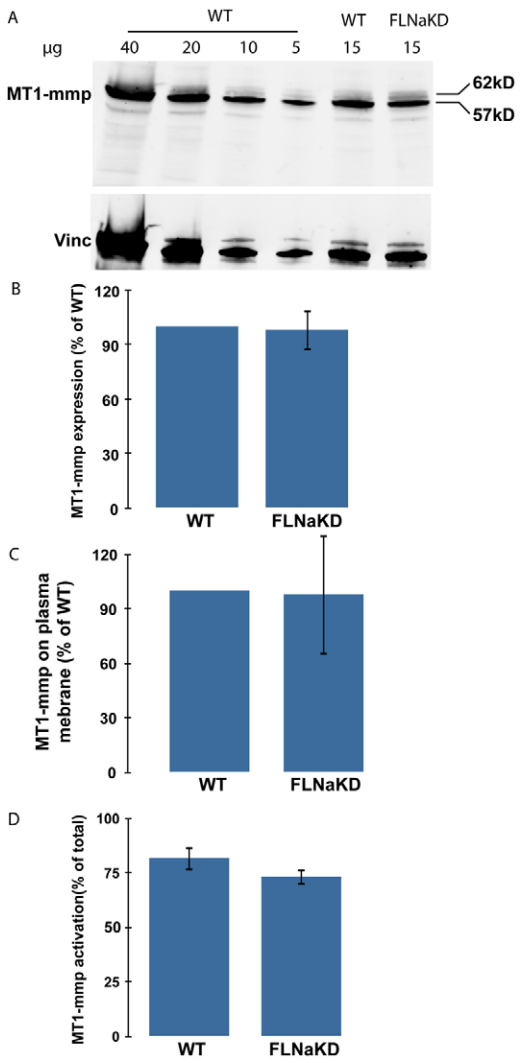

Fig. 6. MT1 processing and membrane levels are not affected by FLNa knockdown. (**A**) HT1080 WT or FLNaKD cells were lysed in RIPA buffer, and lysates were fractionated by SDS-PAGE. After western blotting, samples were probed with anti-MT1-MMP (upper panel) or vinculin (as a loading control; lower panel) antibody. Increasing amounts of WT HT1080 cell lysate were loaded to provide a reference curve allowing careful comparison of protein expression levels. Pro-MT1-MMP (62 kDa) and mature MT1-MMP (57 kDa) are indicated based on the molecular mass. (**B**) Quantification of the total amount of MT1-MMP (pro+mature) in WT or FLNaKD HT1080 cells. In each experiment the amount in the FLNaKD cells was normalized to MT1-MMP in WT cells. The plot shows the mean (±s.e.m.) of six different experiments. (**C**) HT1080 WT or FLNaKD cells were detached and stained on ice with anti-MT1-MMP antibody and subjected to cytofluorometry to detect the amount of cell surface MT1-MMP. The plot shows the mean (±s.e.m.) of six different experiments. (**D**) HT1080 WT or FLNaKD cells were lysed in RIPA buffer, immunoblotted with anti-MT1-MMP antibodies and the percentage of MT1-MMP activation was calculated by dividing the intensity of the 57 kDa band (mature) by the total amount of MT1-MMP [sum of the mature MT1-MMP and pro-MT1-MMP (62 kDa) bands]. The plot shows the mean (±s.e.m.) of six different experiments.

MMPs, impairing MMP2 activation, while low TIMP-2 levels favor MMP2 activation, and a complete lack of TIMP-2 strongly impairs MMP2 activation but favors MT1-MMP activity (Sato and Takino, 2010). Since FLNaKD cells do not appear to have any alteration in MT1-MMP expression/processing, we examined the levels of TIMP-2 in HT1080 WT and FLNaKD cells. As shown in Fig. 7A, FLNaKD and FLNbKD cells have a significant reduction in secreted TIMP-2 without major change in the intracellular levels (Fig. 7B). Importantly the normal levels of secreted TIMP-2 were re-established in FLNaKD cells that re-express FLNa. These findings suggest that the increased MMP2 activation, and an overall increase in MMP activity, may be due to a reduction in TIMP-2 secretion resulting in reduced MMP inhibition and the low TIMP-2 concentrations that maximize MMP2 activation.

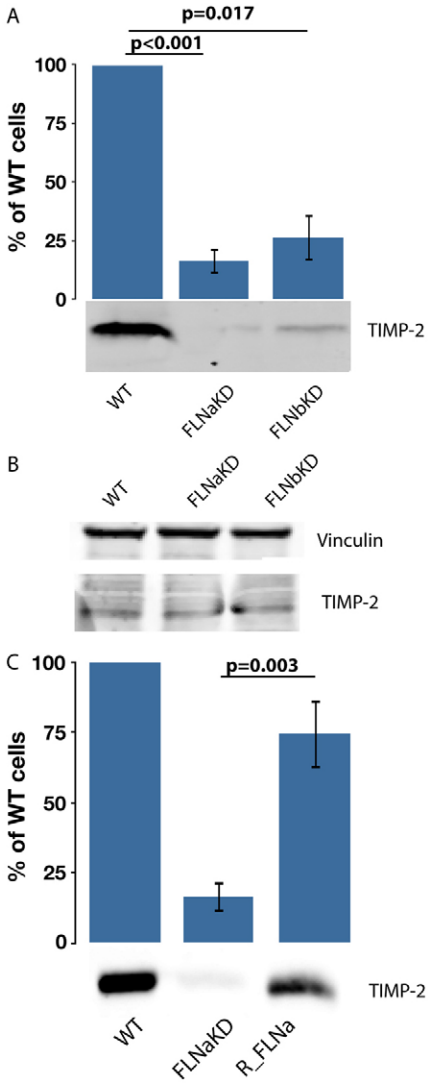

Fig. 7. FLN knockdown reduces TIMP-2 secretion. HT1080 wild-type (WT), FLNaKD or FLNbKD cell-conditioned media (**A**) or cell lysates (**B**) were fractionated by SDS-PAGE and immunoblotted for TIMP-2. Vinculin was used as a loading control and as a control for the number of cells in the well. TIMP-2 levels were quantified and expressed as a percentage of the wild-type cell signal. (**C**) TIMP-2 levels in medium conditioned by HT1080 WT cells, FLNaKD cells or a FLNaKD line re-expressing FLNa (R_FLNa) were assessed and quantified as in A. Plots show mean (±s.e.m.) of at least four independent experiments.

Journal of Cell Science

The filamin A actin-binding domain (FLNa ABD) is required but not sufficient to rescue the degradation phenotype in FLNaKD HT1080 cells

Our data indicate that FLNa knockdown enhances MMP-dependent matrix degradation and increases MMP2 activation. To further characterize the role of FLNa in ECM remodeling we transiently re-expressed GFP-tagged knockdown-resistant FLNa constructs in HT1080 FLNaKD cells and assessed degradation of fluorescent gelatin. Degradation events under the FLNa-re-expressing GFP-positive cells could be compared to those under the untransfected FLNaKD cells plated on the same coverslip. As shown in Fig. 8A, and quantified in 8C, cells that express FLNa-GFP degrade less gelatin, with a 60% reduction in degradation area, while as expected GFP expression does not significantly affect gelatin degradation (Fig. 8C). This observation confirms our earlier finding that the enhanced matrix degradation in FLNaKD cells is FLNa-dependent and suggests that, despite the fact that MMP2 activation could be detected in conditioned medium, there is a cell specific effect due to the pericellular increase in MMP2 activation.

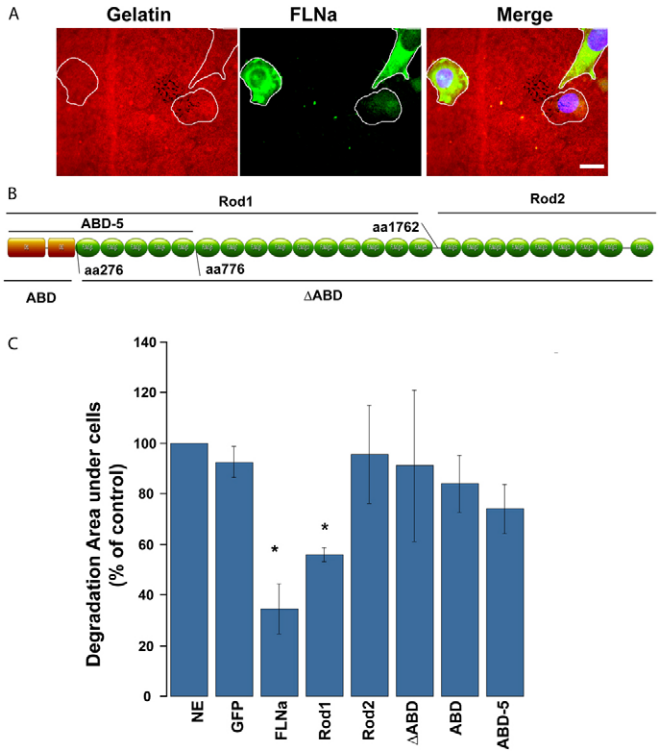

Fig. 8. The FLNa Rod1 domain is required and sufficient to inhibit ECM degradation. (**A**) FLNaKD HT1080 cells were transiently transfected with knockdown-resistant FLNa*GFP; 24 hours later cells were re-plated on fluorescent gelatin, incubated for an additional 4 hours and imaged. Gelatin is shown in red, FLNa*GFP in green and nuclei in blue (in the merge). Cell contours were rendered in white to show cell positions. Scale bars: 20 μm. (**B**) Schematic representation of full-length FLNa. Segments indicate the domains used in C. The boundaries are indicated by amino acid (aa) number. (**C**) FLNaKD HT1080 cells were transiently transfected with the indicated constructs, re-plated after 24 hours cells on fluorescent gelatin for an additional 4 hours and imaged. ECM degradation by the transfected cells was normalized to non-expressing (NE) cells on the same coverslip (results are mean ± s.e.m.; $n>100$ from at least three independent experiments).

To identify filamin A domains important for its effect on matrix degradation, we transfected FLNaKD cells with two non-overlapping FLNa portions: Rod1 or Rod2 (Fig. 8B). Rod1 retains the actin-binding domain (FLNaABD) and the first 15 IgFLN domains while Rod2 contains the final 9 IgFLN domains including the dimerization domain, the major integrin-binding site, and the binding sites for most known FLNa partners. As shown in Fig. 8C, while Rod1 was able to rescue the phenotype in a manner that was statistically indistinguishable from full-length FLNa, Rod2 was completely ineffective. We further asked whether the F-actin binding domain within Rod1 was necessary to reverse the FLNaKD phenotype. As shown in Fig. 8C, expression of a FLNa construct lacking the actin-binding domain (ΔABD) had no effect on gelatin degradation by FLNaKD cells. Hence, the FLNa actin-binding domain is required for the inhibition of gelatin degradation. However, while expression of the ABD by itself appears to slightly reduce ECM degradation, even after analysis of more than 200 transfected cells this effect is not significantly different from non-ABD-expressing FLNaKD cells present on the same coverslip ($P=0.18$), and degradation in ABD expressing cells is significantly greater than in cells re-expressing FLNa ($P=0.03$). We therefore conclude that while the ABD is necessary, it is not sufficient to inhibit ECM degradation in FLNaKD cells (Fig. 8C). Furthermore, gelatin degradation in cells expressing a fragment containing the ABD and the first 5 IgFLNa domains (ABD-5) is indistinguishable from that in cells expressing the ABD alone (Fig. 8C). Taken together our data suggest that to negatively regulate ECM degradation, FLNa needs to bind F-actin and presumably requires some additional interactions mediated via IgFLNa domains 5–15. However, neither FLN dimerization nor integrin binding seem to be required as these occur via IgFLNa domains in the rod 2 region.

Filamin knockdown increases HT1080 cell invasion

The ability to remodel the ECM is an important component of tumor cell invasion and dissemination. We thus tested the role of FLNa in cell invasion in a trans-well assay. These assays have been used extensively to measure the ability of tumor cells to invade an ECM (Kleinman and Jacob, 2001) and recapitulate the two main features that tumor cells require to invade: migration and matrix remodeling. Consistent with our earlier studies (Baldassarre et al., 2009) (supplementary material Fig. S1), when the cells were plated on trans-well filters in the absence of gelatin, such that the only parameter measured is cell motility, no statistically significant differences in migration were found between the wild-type and FLNaKD cells (Fig. 9A). However, if the filters were coated with cross-linked gelatin prior to plating the cells the invasion of WT cells was reduced to near zero, while the HT1080 FLNaKD were still able to migrate at a rate 7 fold higher than that found in WT cells (Fig. 9B). More importantly, the FLNaKD cell migration through gelatin-coated filters was clearly MMP-dependent as invasion was completely abrogated by the broad-spectrum MMP inhibitor GM6001 (Fig. 9B). Taken together, these data show that the removal of FLNa increases the ability of HT1080 cells to invade the surrounding ECM by increasing MMP2 activation and enhancing ECM degradation without directly affecting cell motility.

Discussion

Filamins are essential actin-binding proteins that, in addition to bundling actin filaments, are known to link cell surface adhesion

Journal of Cell Science

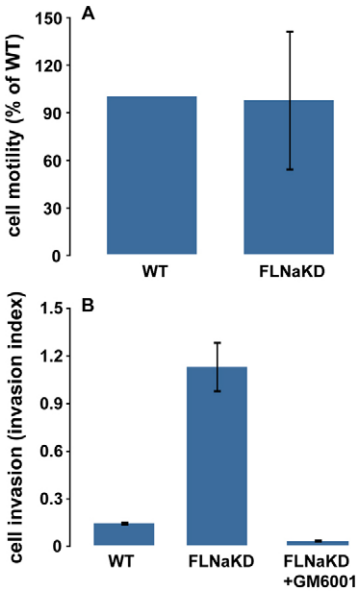

Fig. 9. FLNa knockdown increases HT1080 cell invasion. (**A**) WT or FLNaKD HT1080 cells were detached and plated on 10 mm diameter (8 μm pore size) tissue culture inserts. Cells were allowed to chemotax towards conditioned medium for 5 hours, then fixed and stained with DAPI, then cells in the lower side were imaged at the microscope and quantified. The number of FLNaKD HT1080 cells was normalized to the number of WT cells. The plot shows means±s.e.m. (n=5). (**B**) Cells were treated as in A, but the inserts were coated with cross-linked gelatin (20 mg/ml) prior to cell addition. Where indicated, 150 μm GM6001 was added to both chambers. The plot shows the mean and the 95% confidence interval (n=166 in six independent experiments for WT and FLNaKD cells; n=60 in three independent experiments for cells treated with GM6001).

proteins, signaling receptors, and channels to the actin cytoskeleton, and serve as scaffolds for an array of intracellular signaling proteins (Zhou et al., 2010; Nakamura et al. 2011). The wide range of filamin interactions and activities is reflected in the diversity of disease phenotypes associated with mutations in filamins. Null mutations in *FLNA* lead to the neuronal migration disorder periventricular heterotopia, while filamin mis-sense mutations have been described as determinant of a group of syndromes characterized by skeletal dysplasia and various combinations of cardiac, craniofacial and intestinal anomalies. Among the known functions it is established that filamins can regulate the actin cytoskeleton (Vadlamudi et al., 2002; Flanagan et al., 2001), they have a variety of roles in cell motility (Baldassarre et al., 2009; Calderwood et al., 2001; Cunningham et al., 1992), they are mechanosensors that modulate tissue responses to matrix density (Razinia et al., 2012; Gehler et al., 2009; Ehrlicher et al., 2011), and they negatively regulate the activation of integrin adhesion receptors (Kiema et al., 2006; Ithychanda et al., 2009; Das et al., 2011). In this study we show that the reduction of filamin expression decreases TIMP-2 secretion, increases MMP2 activation, enhances the ability of cells to remodel the ECM and increases their invasive potential. This suggests that filamin normally suppresses ECM degradation and cell invasion. We further show that the actin-binding domain of FLNa is required, but not sufficient, to reverse the increased degradation observed in FLNaKD cells. Perhaps more surprisingly we found that the integrin-binding (Kiema et al., 2006) and the dimerization domains (Gorlin et al., 1990; Pudas et al., 2005) are not required to rescue the FLNaKD phenotype. Our work establishes that, despite being mainly considered as intracellular cytoskeletal signaling adaptors, filamins can regulate the activation of extracellular enzymes and thus affect ECM remodeling with direct consequences on cell invasion. Our findings broaden the range of processes that might be modified in filamin mutant cells or organisms and may provide an explanation for the recent observations that loss of FLNa correlates with increased metastatic potential (Xu et al., 2010; Caruso and Stemmer, 2011).

Research on filamins has often focused on their roles in cell motility and actin dynamics. A range of biochemical, cell-based and in vivo studies have reported a requirement for filamins for normal cell migration (Feng and Walsh, 2004), although in some cases defects in migration were not evident following loss of a single FLN isoform (Baldassarre et al., 2009; Lynch et al., 2011; Hart et al., 2006; Feng et al., 2006). Considering these findings, recent reports that FLNa expression negatively correlates with metastatic potential in breast cancer (Xu et al., 2010; Caruso and Stemmer, 2011) were surprising. Tumor cell dissemination, however, is a complex process that depends on both migration and the ability to cross physical barriers composed of ECM components. Thus, in simple terms, cells could increase their invasive potential by increasing their motility and/or their ability to degrade the surrounding ECM. Our data indicate that knockdown of FLNa or FLNb enhances matrix degradation without detectably altering random cell migration. This raises the possibility that altered ECM turnover may contribute to the enhanced invasion in tumor cells with low FLNa levels.

We find that the enhanced ECM degradation observed in FLNaKD cells is dependent on metalloproteinases as degradation is inhibited by a broad-specificity metalloproteinase inhibitor, GM6001. Furthermore, activation of both cell-derived and serum-derived MMP2 is enhanced in FLNaKD cells and re-expression of FLNa returns both MMP2 activity and ECM degradation to wild-type levels. We did not detect activated MMP9 in our cells (Figs 4, 5), nor MMP1 activity using casein zymography (not shown), so while our results strongly suggest that the enhanced matrix degradation is mediated by MMP2 we cannot exclude the involvement of other MMPs in the process. Indeed, while to our knowledge this is the first report linking FLNa expression to MMP activity, in human melanoma cells FLNa has been reported to negatively regulate MMP9 expression via the Ras/Raf-1/Erk pathway (Zhu et al., 2007). Consistent with this, an increase of MMP9 expression was reported in *FLNA*$^{-/-}$ platelets (Jurak Begonja et al., 2011). Thus, while we did not observe alterations in the levels of secreted MMP9 or MMP2 in HT1080 cells, loss of filamin expression is now associated with increased activation or expression of MMPs in several cell types. Conversely, in macrophages FLNa localizes to and stabilizes podosomes thus enhancing ECM degradation (Guiet et al., 2012), indicating that the effect of filamin on matrix degradation is cell type specific.

MMP2 is normally activated by membrane-type MMPs (MT-MMPs) (Ra and Parks, 2007), the most important of which is MT1-MMP. We did not detect any major change in MT1-MMP expression, maturation, or plasma membrane expression following loss of FLNa (Fig. 7). We therefore conclude that, while MT1-MMP may still be important for MMP2 activation, the loss of FLNa is unlikely to exert its effect via alteration of

Journal of Cell Science

MT1-MMP expression, processing or localization. Likewise, while MMP2–αvβ3 integrin interactions have been implicated in regulation of MMP2 (Brooks et al., 1998; Brooks et al., 1996) cell surface αvβ3 levels are unchanged in FLNaKD and FLNbKD cells (data not shown). However, MMP2 activation is a complex process that depends on the balance between the amount of MMP2, MT1-MMP and tissue inhibitor of metalloproteinase-2 (TIMP-2). Appropriate levels of extracellular TIMP-2 enhance proMMP2 activation (Cao et al., 1996; Strongin et al., 1995), while excess TIMP-2 blocks activation (Cao et al., 1995; Imai et al., 1996; Itoh et al., 2001; Strongin et al., 1995; Toth et al., 2000; Ward et al., 1994; Worley et al., 2003). Analysis of TIMP-2 secretion, revealed a large decrease, but not a complete ablation, of TIMP-2 levels in cell media conditioned by FLN knockdown cells (Fig. 7). This loss of TIMP-2 may explain the observed general increase in MMP activity, and the increase in MMP2 activation in particular. Little is known about regulation of TIMP-2 secretion making it difficult to place our finding in a larger framework; we can hypothesize, however, that FLN directly regulates TIMP-2 secretion. The idea that FLNa could regulate membrane trafficking, while not completely new (Liu et al., 1997), is intriguing especially considering that null mutations in either FLNa or the trafficking related gene ARFGEF2 both cause periventricular heterotopias (Lu et al., 2006). Nonetheless, FLNa deficiency clearly does not result in a general membrane trafficking defect as MMP2 and MMP9 secretion and β1 and β3 integrin surface expression are normal in filamin knockdown cells. We note that TIMP-2 levels might also be reduced by increasing endocytosis of secreted TIMP-2. The fate of TIMP-2 after MMP2 activation is controversial but it has been proposed that the TIMP-2–MT1-MMP complex is endocytosed and degraded (Maquoi et al., 2000), although others suggest that TIMP-2 is released into the medium after breakdown of the ternary MMP2–TIMP-2–MT1-MMP complex (Zucker et al., 2004). Regardless of the exact mechanism, our data clearly show that loss of FLNa or FLNb reduces extracellular TIMP-2 levels.

Many of our studies rely on knockdown cell lines, which offer the convenience of stable populations and the ability to rescue phenotypes by re-expressing knockdown-resistant FLN. Using both stably rescued lines and transient re-expression we have confirmed that the observed phenotypes are due to loss of FLNa and cannot be ascribed to clonal differences. Furthermore, the fact that independent FLNaKD and FLNbKD lines show related phenotypes greatly strengthens our conclusions. While the detailed mechanisms by which loss of filamin enhances ECM degradation remain to be determined, transient re-expression studies have revealed a requirement for FLNa ABD and IgFLNa domains 1–15 in the suppression of ECM degradation. The fact that ECM degradation is suppressed by expression of a FLNa truncation mutant lacking rod2, the region containing both the dimerization domain (Gorlin et al., 1990; Pudas et al., 2005) and the major integrin binding sites (Kiema et al., 2006), seems to exclude a role for FLNa-mediated actin cross-linking or integrin linkage in this process. The actin-binding domain and IgFLNa domains 1–15 are however required. We note that IgFLNa domains 9–15 have been shown to cooperate with the ABD to increase F-actin binding (Nakamura et al., 2007). Whether this, or other IgFLN domain-mediated interactions, are responsible for the inhibition of ECM degradation will be the subject of future studies.

In summary, we have shown that loss of FLNa or FLNb increases ECM degradation without significantly altering two-dimensional random cell migration. Increased ECM degradation correlates with decreased extracellular TIMP-2, increased MMP2 activation, and enhanced cell invasion. We suggest that filamins normally act to suppress ECM degradation and that this depends on the N-terminal actin-binding domain of the filamins as well as the first 15 IgFLN domains. Finally, our data indicate that effects on ECM remodeling and cell invasion should be considered when attempting to provide cellular explanations for the physiological and pathological effects of altered FLN expression or FLN mutations.

Materials and Methods

Reagents and DNA constructs

Monoclonal anti-vinculin antibody (Sigma), monoclonal anti-TIMP-2 (Abcam), monoclonal anti-MT1-MMP (Millipore), polyclonal anti-GFP (Rockland), monoclonal anti-FLNa (Abcam), polyclonal anti-FLNb (Millipore LOT#0601019666), secondary anti-rabbit and anti-mouse HRP-conjugated (GE Healthcare), anti mouse Alexa-568, anti-rabbit and anti-goat Alexa-680 conjugated (Invitrogen, Carlsbad, CA), anti-mouse FITC conjugated (Pierce, Rockford, IL), anti-mouse IRDye 800 (LI-COR Biotechnology, Lincoln NB), and DAPI (Sigma) were purchased. Anti-FLNa and anti-FLNb anti-serum raised against the domains 19 to 21 of the respective proteins were previously described (Baldassarre et al., 2009; Kiema et al., 2006). FLNa-GFP, Rod2-GFP and FLNaABD as well as shRNA-resistant FLNa*GFP, expression constructs were previously described (Baldassarre et al., 2009; Lad et al., 2007, Lad et al., 2008; Razinia et al., 2011). FLNaABD-5 was generated by PCR and subcloned into GFP pCDNA3. shRNA resistant Rod1*GFP and FLNa*ΔABD were generated with the QuikChange site-directed mutagenesis kit (Stratagene) from the constructs used in Razinia et al. (Razinia et al., 2011) and confirmed by DNA sequencing. FLN-targeting shRNAs in the pSM2c and pGIPZ vectors were purchased from OpenBiosystems. GM6001(calbiochem) and the MMP substrate Mca-Pro-Leu-Gly-Dpa-Ala-Arg-NH2 (Novabiochem) were kindly provided by Ben Turk (Yale University).

Cell culture

Human fibrosarcoma HT1080 cells were cultured in Dulbecco's Modified Essential Medium (Invitrogen) containing 9% fetal bovine serum (Atlanta Biological, Lawrenceville, GA) and penicillin/streptomycin (Invitrogen) and incubated at 37℃ in a humidified atmosphere containing 5% CO_2.

Generation of FLN knockdown cell lines

Polyclonal HT1080 FLNa knockdown cell lines were previously described (Baldassarre et al., 2009). Briefly, HT1080 wild-type cells were transfected with pSM2 vector expressing FLNa shRNA or FLNbs shRNA in pGIPZ and selected using 2 μg/ml Puromycin (Sigma). Single clone lines were obtained by limiting dilution of the polyclonal population. Single clones were screened for FLNa content by immunofluorescence staining with FLN antibodies in 96 well plates and the signal quantified on a fluorescence plate reader (Safire). To correct for well to well variation in cell number the FLN signal was normalized to actin.

Quantification of FLN expression levels

To quantify FLN expression in the knockdown cells increasing amounts of lysate from WT cells were fractionated alongside knockdown lysates on SDS-PAGE and after western blotting probed with anti-FLNa and/or anti-FLNb antibodies and anti-vinculin antibodies as loading controls. Membranes were scanned using the Odyssey infrared imaging system. The signals were quantified using ImageJ, and FLN knockdown calculated according to the standard curve generated from the WT lysates after correction for loading using the vinculin signals.

Immunofluorescence

Cells, seeded on either FN-coated coverslips or 3.5 cm Petri dishes (Becton Dickinson), were fixed in 4% paraformaldehyde in phosphate buffered saline (PBS) pH 7.4 for 15 minutes and permeabilized for 30 minutes with PBS containing 0.02% saponin, 0.2% bovine serum albumin (BSA) and 50 mM NH_4Cl. Cells were then incubated with DAPI and primary antibodies of interest for 1 hour at room temperature, then, when necessary, incubated with fluorophore-conjugated secondary antibodies for 45 minutes washed again in PBS and coverslips were mounted using the ProLongGold anti-fade mounting agent (Invitrogen). Images were acquired on a Nikon TE2000 with a 10× or 40× objective using IPLab (version 3.5.2; Scanalytics, Fairfax, VA) software and analyzed using ImageJ (U. S. National Institutes of Health, Bethesda, MD, http://rsb.info.nih.gov/ij/; versions 1.42-1.46A).

Journal of Cell Science

Immunoblotting

Cells were lysed in RIPA buffer (0.35 M Tris pH 7.2, 0.5 M NaCl, 10 mM $MgCl_2$, 1% Triton X-100, 0.1% SDS, 0.5% Sodium Deoxicolate) containing Protease Inhibitors Cocktail Tablets (Roche). Lysates were run on SDS-PAGE, transferred onto nitrocellulose membrane, blocked for 1 hour with 5% not-fat milk in T-TBS (0.1 M Tris pH 7.4, 135 mM NaCl, 0.05% Tween-20). Membranes were probed 1 hour at room temperature or overnight at 4℃ with primary antibody, washed in T-TBS and incubated for 1 hour with fluorescent secondary antibodies. Signal was detected using the Odyssey infrared imaging system (LI-COR Biotechnology).

ECM degradation assay

Fluorescent matrix-coated coverslips were prepared and the assay carried out as described previously (Baldassarre et al., 2006). Briefly, thin layers of, fluorescein- or rhodamine B- (Sigma) conjugated gelatin (Sigma) (5 mg/ml) were placed on coverslips, cross-linked with 0.5% glutaraldehyde for 15 minutes at 0℃, and washed three times with phosphate-buffered saline (PBS). Finally, after a wash in PBS and 10-minute incubation in 70% ethanol, coverslips were quenched with complete medium for 1 hour at 37℃ before cell plating.

ECM degradation quantification

Cells plated on fluorescent ECM were fixed at the indicated time with 4% paraformaldhyde in PBS for 15 minutes at 37℃, permeabilized for 30 minutes with PBS containing 0.02% saponin, 0.2% bovine serum albumin (BSA) and 50 mM NH_4Cl and nuclei were stained with DAPI 0.5 μg/ml. After mounting the coverslip using ProLongGold anti-fade mounting agent, microscopic fields were acquired randomly using PriorScan automatic XY stage coupled to a Nikon eclipse Ti and controlled by MicroManger open source software (Edelstein et al., 2010). All the fieds were acquired using a 40× magnification and one EXi-blue CCD camera with a 2× binning (final pixel size=0.3225 μm). The degradation areas were then quantified with a custom ImageJ macro with the follow algorithm: first, nuclei were identified in the blue (DAPI) channel assuming a bimodal distribution were the lower (dark) modal value represented the background and the higher one (brighter) represented the nuclei, the threshold was then placed at the intermodal value. Second, on the red (ECM) channel regions of interest encompassing the area under the cell and its immediate surrounding were selected by extending 50 pixels around the perimeter of each nucleus). Finally, degradations (regions with low ECM fluorescence) in the regions of interest were identified as pixels with a value $v<m-3d$, where m is the modal value and d the standard deviation of the fluorescence in the specified region of interest. To reduce noise an additional tresholding was added to remove all the degradations that were smaller than 5 pixels. In transient transfection experiments, expressing cells were identified by measuring the green fluorescence in a 10 pixels wide ring around the nuclei, cells were considered 'green' (i.e. transfected) if their fluorescent value $v>M+2d$, where M is the mean value of all the measured cells and d is the standard deviation of the population.

Zymography

Cells plated in 10 cm plates were incubated with 5 ml of Dulbecco's Modified Essential Medium, after 24 hours the media were harvested and concentrated to the final volume of 500 μl. 20 μl of this concentrated medium were then added with 4 μl of sample buffer 4× (without reducing agents) and loaded on a 10% SDS-PAGE gel containing 1 mg/ml gelatin. After separation, the gels were washed three times in 2.5% Triton X-100 to remove the SDS and incubated for 15 hours at 37℃ in developing buffer (10 mM $CaCl_2$ in 50 mM Tris pH 7.4). The gel was then stained with Coomassie blue and the activity was quantified measuring the negative bands (i.e. the non-blue stained parts of the gel).

To ensure that signals did not reach saturation we also performed real time Zymography using 10% SDS-PAGE gel containing 1 mg/ml FITC-gelatin. After separation, the gels were washed three times in 2.5% Triton X-100 to remove the SDS and incubated at 37℃ and imaged under UV light at different time points. In all the experiments we performed saturation occurred between 24 and 48 hours after the start of the incubation, indicating that the measurements at 15 hours were taken well before saturation.

Cytofluorometry

Cells were detached in trypsin EDTA, washed twice in PBS, then incubated for 30 minutes at 0℃ with anti-MT1-MMP, washed twice in PBS, incubated for other 30 minutes at 0℃ with anti-mouse FITC conjugated, washed twice in PBS and analysed using FACS Calibur machine (BD Bioscience).

Time-lapse migration assays

Migration assays were performed as described previuosly (Baldassarre et al., 2009). Briefly, cells were washed, detached and plated on 5 μg/ml gelatin coated non-tissue culture treated 3.5 cm dishes. Grids were etched on the bottom of the plate to aid location of cells following staining. Both control and knockdown cells were seeded in the same dish. Ten minutes after plating, unattached cells were removed by washing. Starting 1 hour after plating cells were imaged by phase contrast every 5 minutes for 4 hours, on a Nikon TE2000 with a 20× objective. For each experiments at least three fields from the same plate were acquired using an automated PriorScan XY stage. The cells were kept at 37℃ using a home-designed thermostatic chamber. Cells were then fixed with 4% PFA for 15 minutes and immuno-fluorescence staining for FLNa was performed. Cells in the imaged field were identified and FLN levels were measured using ImageJ by multiplying the mean fluorescence, corrected for the background, by the area of the cell. Analysis of the track of each cell in the field was quantified by manual rendering of the nuclear profile in all frames allowing localization of the coordinates of the nucleus centroid and calculation of path length, displacement from origin, and average speed (total path length/time).

MMP activity assay

Cells were plated in glass 96 well plate (black walls, Becton Dickinson), allowed to adhere for one night, then washed three times in Medium 199 (Invitrogen) without serum and incubated at 37℃ in 150 μl of the same medium. After 3 hours the flurogenic MCA-Pro-Leu-Gly-Leu-Dpa-Ala-Arg-NH2 substrate was added at 5 μM final concentration plus or minus the MMP inhibitor GM6001 at 100 μM final concentration. This MMP substrate was first described by Knight and colleagues (Knight et al., 1992) and is widely used as a general MMP substrate. The increasing MCA fluorescence was measured every minute for 30 minutes. To determine specific activity, the fluorescence of samples containing the MMP inhibitor was subtracted at each time point and the data used to generate a trend-line. The slope of that linear regression was averaged between replicates.

Trans-well migration/invasion assay

To measure migration, cells were detached, washed and resuspended (10^6/ml) in fresh complete medium. 200 μl of the cell suspension were then plated onto 10 mm diameter (8 μm pore size) tissue culture inserts (Nunc). Conditioned medium was added to the lower chamber and cells were allowed to chemotax towards it for 5 hours. Cells were then fixed, stained with DAPI. Cells in the upper chamber were removed, those in the lower side were imaged at the microscope and quantified. For each experimental condition (run in duplicate) 20 random fields were acquired. The number of FLNaKD HT1080 cells that migrated to the lower surface was then normalized to the number of WT ones in the same experiment. Cell invasion assays were performed similarly to the migration assays but prior to cell addition the inserts were coated with cross-linked gelatin (20 mg/ml). The number of invading cells was normalized to the number of cells that migrated to the lower side of the field in the absence of gelatin coating (invasion index).

Acknowledgements

We thank Ben Turk for advice and for providing tools for the MMP assays and Mariagrazia Capestrano for fruitful discussions.

Funding

This work was supported by grants from National Institutes of Health [grant numbers RO1 GM-068600, T32 GM-007223]; an award from American Heart Association to Z.R.; and by awards from the Italian Association for Cancer Research (AIRC); and the European Union's Seventh Framework Program [grant agreement number 237946 to R.B.]. Deposited in PMC for release after 12 months.

Supplementary material available online at
http://jcs.biologists.org/lookup/suppl/doi:10.1242/jcs.104018/-/DC1

References

Baldassarre, M., Pompeo, A., Beznoussenko, G., Castaldi, C., Cortellino, S., McNiven, M. A., Luini, A. and Buccione, R. (2003). Dynamin participates in focal extracellular matrix degradation by invasive cells. *Mol. Biol. Cell* **14**, 1074-1084.

Baldassarre, M., Ayala, I., Beznoussenko, G., Giacchetti, G., Machesky, L. M., Luini, A. and Buccione, R. (2006). Actin dynamics at sites of extracellular matrix degradation. *Eur. J. Cell Biol.* **85**, 1217-1231.

Baldassarre, M., Razinia, Z., Burande, C. F., Lamsoul, I., Lutz, P. G. and Calderwood, D. A. (2009). Filamins regulate cell spreading and initiation of cell migration. *PLoS ONE* **4**, e7830.

Bourboulia, D. and Stetler-Stevenson, W. G. (2010). Matrix metalloproteinases (MMPs) and tissue inhibitors of metalloproteinases (TIMPs): Positive and negative regulators in tumor cell adhesion. *Semin. Cancer Biol.* **20**, 161-168.

Brooks, P. C., Strömblad, S., Sanders, L. C., von Schalscha, T. L., Aimes, R. T., Stetler-Stevenson, W. G., Quigley, J. P. and Cheresh, D. A. (1996). Localization of matrix metalloproteinase MMP-2 to the surface of invasive cells by interaction with integrin alpha v beta 3. *Cell* **85**, 683-693.

Brooks, P. C., Silletti, S., von Schalscha, T. L., Friedlander, M. and Cheresh, D. A. (1998). Disruption of angiogenesis by PEX, a noncatalytic metalloproteinase fragment with integrin binding activity. *Cell* **92**, 391-400.

Journal of Cell Science

Calderwood, D. A., Huttenlocher, A., Kiosses, W. B., Rose, D. M., Woodside, D. G., Schwartz, M. A. and Ginsberg, M. H. (2001). Increased filamin binding to β-integrin cytoplasmic domains inhibits cell migration. *Nat. Cell Biol.* **3**, 1060-1068.

Cao, J., Sato, H., Takino, T. and Seiki, M. (1995). The C-terminal region of membrane type matrix metalloproteinase is a functional transmembrane domain required for pro-gelatinase A activation. *J. Biol. Chem.* **270**, 801-805.

Cao, J., Rehemtulla, A., Bahou, W. and Zucker, S. (1996). Membrane type matrix metalloproteinase 1 activates pro-gelatinase A without furin cleavage of the N-terminal domain. *J. Biol. Chem.* **271**, 30174-30180.

Caruso, J. A. and Stemmer, P. M. (2011). Proteomic profiling of lipid rafts in a human breast cancer model of tumorigenic progression. *Clin. Exp. Metastasis* **28**, 529-540.

Cunningham, C. C., Gorlin, J. B., Kwiatkowski, D. J., Hartwig, J. H., Janmey, P. A., Byers, H. R. and Stossel, T. P. (1992). Actin-binding protein requirement for cortical stability and efficient locomotion. *Science* **255**, 325-327.

Das, M., Ithychanda, S. S., Qin, J. and Plow, E. F. (2011). Migfilin and filamin as regulators of integrin activation in endothelial cells and neutrophils. *PLoS ONE* **6**, e26355.

Edelstein, A., Amodaj, N., Hoover, K., Vale, R. and Stuurman, N. (2010). Computer control of microscopes using microManager. *Curr. Protoc. Mol. Biol.* Chapter **14**, Unit14.

Ehrlicher, A. J., Nakamura, F., Hartwig, J. H., Weitz, D. A. and Stossel, T. P. (2011). Mechanical strain in actin networks regulates FilGAP and integrin binding to filamin A. *Nature* **478**, 260-263.

Feng, Y. and Walsh, C. A. (2004). The many faces of filamin: a versatile molecular scaffold for cell motility and signalling. *Nat. Cell Biol.* **6**, 1034-1038.

Feng, Y., Chen, M. H., Moskowitz, I. P., Mendonza, A. M., Vidali, L., Nakamura, F., Kwiatkowski, D. J. and Walsh, C. A. (2006). Filamin A (FLNA) is required for cell-cell contact in vascular development and cardiac morphogenesis. *Proc. Natl. Acad. Sci. USA* **103**, 19836-19841.

Flanagan, L. A., Chou, J., Falet, H., Neujahr, R., Hartwig, J. H. and Stossel, T. P. (2001). Filamin A, the Arp2/3 complex, and the morphology and function of cortical actin filaments in human melanoma cells. *J. Cell Biol.* **155**, 511-518.

Fox, J. W. and Walsh, C. A. (1999). Periventricular heterotopia and the genetics of neuronal migration in the cerebral cortex. *Am. J. Hum. Genet.* **65**, 19-24.

Gehler, S., Baldassarre, M., Lad, Y., Leight, J. L., Wozniak, M. A., Riching, K. M., Eliceiri, K. W., Weaver, V. M., Calderwood, D. A. and Keely, P. J. (2009). Filamin A-β1 Integrin Complex Tunes Epithelial Cell Response to Matrix Tension. *Mol. Biol. Cell* **20**, 3224-3238.

Gorlin, J. B., Yamin, R., Egan, S., Stewart, M., Stossel, T. P., Kwiatkowski, D. J. and Hartwig, J. H. (1990). Human endothelial actin-binding protein (ABP-280, nonmuscle filamin): a molecular leaf spring. *J. Cell Biol.* **111**, 1089-1105.

Grobelny, D., Poncz, L. and Galardy, R. E. (1992). Inhibition of human skin fibroblast collagenase, thermolysin, and Pseudomonas aeruginosa elastase by peptide hydroxamic acids. *Biochemistry* **31**, 7152-7154.

Guiet, R., Vérollet, C., Lamsoul, I., Cougoule, C., Poincloux, R., Labrousse, A., Calderwood, D. A., Glogauer, M., Lutz, P. G. and Maridonneau-Parini, I. (2012). Macrophage mesenchymal migration requires podosome stabilization by filamin A. *J. Biol. Chem.* **287**, 13051-13062.

Hart, A. W., Morgan, J. E., Schneider, J., West, K., McKie, L., Bhattacharya, S., Jackson, I. J. and Cross, S. H. (2006). Cardiac malformations and midline skeletal defects in mice lacking filamin A. *Hum. Mol. Genet.* **15**, 2457-2467.

Hartwig, J. H., Tyler, J. and Stossel, T. P. (1980). Actin-binding protein promotes the bipolar and perpendicular branching of actin filaments. *J. Cell Biol.* **87**, 841-848.

Heuzé, M. L., Lamsoul, I., Baldassarre, M., Lad, Y., Lévêque, S., Razinia, Z., Moog-Lutz, C., Calderwood, D. A. and Lutz, P. G. (2008). ASB2 targets filamins A and B to proteasomal degradation. *Blood* **112**, 5130-5140.

Imai, K., Ohuchi, E., Aoki, T., Nomura, H., Fujii, Y., Sato, H., Seiki, M. and Okada, Y. (1996). Membrane-type matrix metalloproteinase 1 is a gelatinolytic enzyme and is secreted in a complex with tissue inhibitor of metalloproteinases 2. *Cancer Res.* **56**, 2707-2710.

Ithychanda, S. S., Das, M., Ma, Y. Q., Ding, K., Wang, X., Gupta, S., Wu, C., Plow, E. F. and Qin, J. (2009). Migfilin, a molecular switch in regulation of integrin activation. *J. Biol. Chem.* **284**, 4713-4722.

Itoh, Y., Takamura, A., Ito, N., Maru, Y., Sato, H., Suenaga, N., Aoki, T. and Seiki, M. (2001). Homophilic complex formation of MT1-MMP facilitates proMMP-2 activation on the cell surface and promotes tumor cell invasion. *EMBO J.* **20**, 4782-4793.

Jurak Begonja, A., Hoffmeister, K. M., Hartwig, J. H. and Falet, H. (2011). FlnA-null megakaryocytes prematurely release large and fragile platelets that circulate poorly. *Blood* **118**, 2285-2295.

Kesner, B. A., Milgram, S. L., Temple, B. R. and Dokholyan, N. V. (2010). Isoform divergence of the filamin family of proteins. *Mol. Biol. Evol.* **27**, 283-295.

Kessenbrock, K., Plaks, V. and Werb, Z. (2010). Matrix metalloproteinases: regulators of the tumor microenvironment. *Cell* **141**, 52-67.

Kiema, T., Lad, Y., Jiang, P., Oxley, C. L., Baldassarre, M., Wegener, K. L., Campbell, I. D., Ylänne, J. and Calderwood, D. A. (2006). The molecular basis of filamin binding to integrins and competition with talin. *Mol. Cell* **21**, 337-347.

Kim, H. and McCulloch, C. A. (2011). Filamin A mediates interactions between cytoskeletal proteins that control cell adhesion. *FEBS Lett.* **585**, 18-22.

Kleinman, H. K. and Jacob, K. (2001). Invasion assays. *Curr. Protoc. Cell Biol.* Chapter **12**, Unit 12.2.

Knight, C. G., Willenbrock, F. and Murphy, G. (1992). A novel coumarin-labelled peptide for sensitive continuous assays of the matrix metalloproteinases. *FEBS Lett.* **296**, 263-266.

Lad, Y., Kiema, T., Jiang, P., Pentikäinen, O. T., Coles, C. H., Campbell, I. D., Calderwood, D. A. and Ylänne, J. (2007). Structure of three tandem filamin domains reveals auto-inhibition of ligand binding. *EMBO J.* **26**, 3993-4004.

Lad, Y., Jiang, P., Ruskamo, S., Harburger, D. S., Ylänne, J., Campbell, I. D. and Calderwood, D. A. (2008). Structural basis of the migfilin-filamin interaction and competition with integrin beta tails. *J. Biol. Chem.* **283**, 35154-35163.

Liu, G., Thomas, L., Warren, R. A., Enns, C. A., Cunningham, C. C., Hartwig, J. H. and Thomas, G. (1997). Cytoskeletal protein ABP-280 directs the intracellular trafficking of furin and modulates proprotein processing in the endocytic pathway. *J. Cell Biol.* **139**, 1719-1733.

Lu, J., Tiao, G., Folkerth, R., Hecht, J., Walsh, C. and Sheen, V. (2006). Overlapping expression of ARFGEF2 and Filamin A in the neuroependymal lining of the lateral ventricles: insights into the cause of periventricular heterotopia. *J. Comp. Neurol.* **494**, 476-484.

Lynch, C. D., Gauthier, N. C., Biais, N., Lazar, A. M., Roca-Cusachs, P., Yu, C. H. and Sheetz, M. P. (2011). Filamin depletion blocks endoplasmic spreading and destabilizes force-bearing adhesions. *Mol. Biol. Cell* **22**, 1263-1273.

Maquoi, E., Frankenne, F., Baramova, E., Munaut, C., Sounni, N. E., Remacle, A., Noël, A., Murphy, G. and Foidart, J. M. (2000). Membrane type 1 matrix metalloproteinase-associated degradation of tissue inhibitor of metalloproteinase 2 in human tumor cell lines. *J. Biol. Chem.* **275**, 11368-11378.

Mazzone, M., Baldassarre, M., Beznoussenko, G., Giacchetti, G., Cao, J., Zucker, S., Luini, A. and Buccione, R. (2004). Intracellular processing and activation of membrane type 1 matrix metalloprotease depends on its partitioning into lipid domains. *J. Cell Sci.* **117**, 6275-6287.

Mueller, S. C. and Chen, W. T. (1991). Cellular invasion into matrix beads: localization of beta 1 integrins and fibronectin to the invadopodia. *J. Cell Sci.* **99**, 213-225.

Nagano, T., Yoneda, T., Hatanaka, Y., Kubota, C., Murakami, F. and Sato, M. (2002). Filamin A-interacting protein (FILIP) regulates cortical cell migration out of the ventricular zone. *Nat. Cell Biol.* **4**, 495-501.

Nakamura, F., Osborn, T. M., Hartemink, C. A., Hartwig, J. H. and Stossel, T. P. (2007). Structural basis of filamin A functions. *J. Cell Biol.* **179**, 1011-1025.

Nakamura, F., Stossel, T. P. and Hartwig, J. H. (2011). The filamins: organizers of cell structure and function. *Cell Adh. Migr.* **5**, 160-169.

Neumann, U., Kubota, H., Frei, K., Ganu, V. and Leppert, D. (2004). Characterization of Mca-Lys-Pro-Leu-Gly-Leu-Dpa-Ala-Arg-NH2, a fluorogenic substrate with increased specificity constants for collagenases and tumor necrosis factor converting enzyme. *Anal. Biochem.* **328**, 166-173.

Popowicz, G. M., Schleicher, M., Noegel, A. A. and Holak, T. A. (2006). Filamins: promiscuous organizers of the cytoskeleton. *Trends Biochem. Sci.* **31**, 411-419.

Pudas, R., Kiema, T. R., Butler, P. J., Stewart, M. and Ylänne, J. (2005). Structural basis for vertebrate filamin dimerization. *Structure. (Camb.)* **13**, 111-119.

Ra, H. J. and Parks, W. C. (2007). Control of matrix metalloproteinase catalytic activity. *Matrix Biol.* **26**, 587-596.

Razinia, Z., Baldassarre, M., Bouaouina, M., Lamsoul, I., Lutz, P. G. and Calderwood, D. A. (2011). The E3 ubiquitin ligase specificity subunit ASB2α targets filamins for proteasomal degradation by interacting with the filamin actin-binding domain. *J. Cell Sci.* **124**, 2631-2641.

Razinia, Z., Makela, T., Ylänne, J. and Calderwood, D. A. (2012). Filamins in mechanosensing and signaling. *Annu. Rev. Biophys.* **41**, 227-246.

Robertson, S. P., Twigg, S. R., Sutherland-Smith, A. J., Biancalana, V., Gorlin, R. J., Horn, D., Kenwrick, S. J., Kim, C. A., Morava, E., Newbury-Ecob, R. et al.; OPD-spectrum Disorders Clinical Collaborative Group (2003). Localized mutations in the gene encoding the cytoskeletal protein filamin A cause diverse malformations in humans. *Nat. Genet.* **33**, 487-491.

Sato, H. and Takino, T. (2010). Coordinate action of membrane-type matrix metalloproteinase-1 (MT1-MMP) and MMP-2 enhances pericellular proteolysis and invasion. *Cancer Sci.* **101**, 843-847.

Stanton, H., Gavrilovic, J., Atkinson, S. J., d'Ortho, M. P., Yamada, K. M., Zardi, L. and Murphy, G. (1998). The activation of ProMMP-2 (gelatinase A) by HT1080 fibrosarcoma cells is promoted by culture on a fibronectin substrate and is concomitant with an increase in processing of MT1-MMP (MMP-14) to a 45 kDa form. *J. Cell Sci.* **111**, 2789-2798.

Stossel, T. P., Condeelis, J., Cooley, L., Hartwig, J. H., Noegel, A., Schleicher, M. and Shapiro, S. S. (2001). Filamins as integrators of cell mechanics and signalling. *Nat. Rev. Mol. Cell Biol.* **2**, 138-145.

Strongin, A. Y., Collier, I., Bannikov, G., Marmer, B. L., Grant, G. A. and Goldberg, G. I. (1995). Mechanism of cell surface activation of 72-kDa type IV collagenase. Isolation of the activated form of the membrane metalloprotease. *J. Biol. Chem.* **270**, 5331-5338.

Toth, M., Bernardo, M. M., Gervasi, D. C., Soloway, P. D., Wang, Z., Bigg, H. F., Overall, C. M., DeClerck, Y. A., Tschesche, H., Cher, M. L. et al. (2000). Tissue inhibitor of metalloproteinase (TIMP)-2 acts synergistically with synthetic matrix metalloproteinase (MMP) inhibitors but not with TIMP-4 to enhance the (Membrane type 1)-MMP-dependent activation of pro-MMP-2. *J. Biol. Chem.* **275**, 41415-41423.

Vadlamudi, R. K., Li, F., Adam, L., Nguyen, D., Ohta, Y., Stossel, T. P. and Kumar, R. (2002). Filamin is essential in actin cytoskeletal assembly mediated by p21-activated kinase 1. *Nat. Cell Biol.* **4**, 681-690.

van der Flier, A. and Sonnenberg, A. (2001). Structural and functional aspects of filamins. *Biochim. Biophys. Acta* **1538**, 99-117.

Ward, R. V., Atkinson, S. J., Reynolds, J. J. and Murphy, G. (1994). Cell surface-mediated activation of progelatinase A: demonstration of the involvement of the C-terminal domain of progelatinase A in cell surface binding and activation of progelatinase A by primary fibroblasts. *Biochem. J.* **304**, 263-269.

Worley, J. R., Thompkins, P. B., Lee, M. H., Hutton, M., Soloway, P., Edwards, D. R., Murphy, G. and Knäuper, V. (2003). Sequence motifs of tissue inhibitor of metalloproteinases 2 (TIMP-2) determining progelatinase A (proMMP-2) binding and activation by membrane-type metalloproteinase 1 (MT1-MMP). *Biochem. J.* **372**, 799-809.

Xu, Y., Bismar, T. A., Su, J., Xu, B., Kristiansen, G., Varga, Z., Teng, L., Ingber, D. E., Mammoto, A., Kumar, R. et al. (2010). Filamin A regulates focal adhesion disassembly and suppresses breast cancer cell migration and invasion. *J. Exp. Med.* **207**, 2421-2437.

Yamazaki, M., Furuike, S. and Ito, T. (2002). Mechanical response of single filamin A (ABP-280) molecules and its role in the actin cytoskeleton. *J. Muscle Res. Cell Motil.* **23**, 525-534.

Zhou, A. X., Hartwig, J. H. and Akyürek, L. M. (2010). Filamins in cell signaling, transcription and organ development. *Trends Cell Biol.* **20**, 113-123.

Zhou, X., Borén, J. and Akyürek, L. M. (2007). Filamins in cardiovascular development. *Trends Cardiovasc. Med.* **17**, 222-229.

Zhu, T. N., He, H. J., Kole, S., D'Souza, T., Agarwal, R., Morin, P. J. and Bernier, M. (2007). Filamin A-mediated down-regulation of the exchange factor Ras-GRF1 correlates with decreased matrix metalloproteinase-9 expression in human melanoma cells. *J. Biol. Chem.* **282**, 14816-14826.

Zucker, S., Hymowitz, M., Conner, C., DeClerck, Y. and Cao, J. (2004). TIMP-2 is released as an intact molecule following binding to MT1-MMP on the cell surface. *Exp. Cell Res.* **293**, 164-174.

Journal of Cell Science

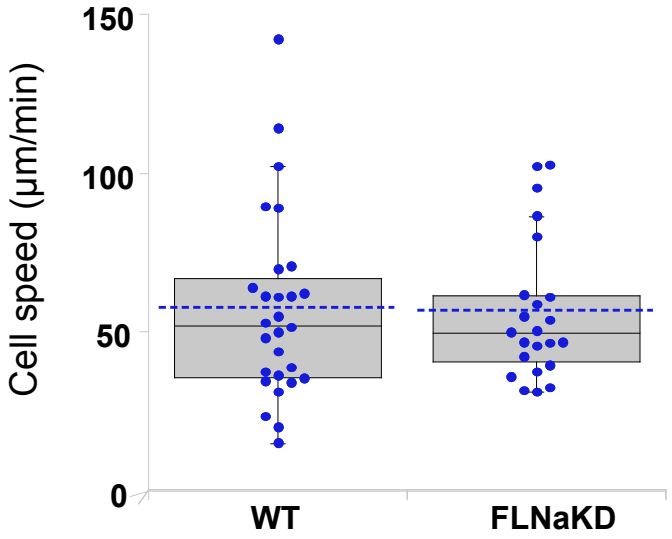

Fig S1. Cell motility and ECM degradation. The speed of migration of HT1080 WT and FLNaKD was compared in time-lapse migration assays on gelatin coated substrates. The dot plot shows the overall population distribution (7 movies were quantified, total sample size: WT = 28; FLNaKD = 23), dotted line shows the mean value, box and whiskers plots show quartiles.